Influence of Chloride Ions on the Synthesis of Colloidal Branched CdSe/CdS Nanocrystals by Seeded Growth

Mee Rahn Kim, Karol Miszta, Mauro Povia, Rosaria Brescia, Sotirios Christodoulou, Mirko Prato, Sergio Marras, and Liberato Manna*

Department of Nanochemistry, Istituto Italiano di Tecnologia, via Morego, 30, 16163 Genova, Italy

ABSTRACT We studied the influence of chloride ions (Cl^-), introduced as $CdCl_2$, on the seeded growth synthesis of colloidal branched CdSe(core)/CdS(pods) nanocrystals. This is carried out by growing wurtzite CdS pods on top of preformed octahedral sphalerite CdSe seeds. When no $CdCl_2$ is added, the synthesis of multipods has a low reproducibility, and the side nucleation of CdS nanorods is often observed. At a suitable concentration of $CdCl_2$, octapods are formed and they are stable in solution during the synthesis. Our experiments indicate that Cl^- ions introduced in the reaction reduce the availability of Cd^{2+} ions in solution, most likely *via* formation of strong complexes with both Cd and the various surfactants. This prevents homogeneous nucleation of CdS nanocrystals, so that the heterogeneous nucleation of CdS pods on top of the CdSe seeds is the preferred process. Once such optimal concentration of $CdCl_2$ is set for a stable growth of octapods, the pod lengths can be tuned by varying the relative ratios of the various alkyl phosphonic acids used. Furthermore, at higher concentrations of $CdCl_2$ added, octapods are initially formed, but many of them evolve into tetrapods over time. This transformation points to an additional role of Cl species in regulating the growth rate and stability of various crystal facets of the CdS pods.

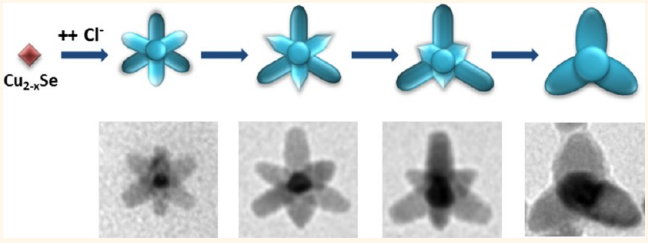

KEYWORDS: branched nanocrystals · colloidal synthesis · seeded growth · impurities · chloride ions · shape control · octapods

Colloidal nanocrystals (NCs), especially those based on semiconductors, find applications in many fields, such as optics, photovoltaics, nanoelectronics, and biosensing.[1−7] The development of well-controlled synthetic methods to NCs and the elucidation of the mechanisms governing their shapes and sizes are important issues in material chemistry.[8−17] The advances that have been made in the last 20 years in the synthesis of colloidal NCs have shown how the kinetics and thermodynamics of nucleation and growth of NCs in solution can be affected by the presence of many impurities.[18−23] Several cases have been reported in which the serendipitous discovery of new NC shapes has sparked research on what chemicals in the reaction environment were actually responsible for the formation of such shapes.[19−24] These studies have shed light on the mechanisms involved in the syntheses of NCs and have helped to formulate more robust synthesis routes to NCs of a wide variety of sizes and shapes. On the other hand, it is not uncommon that many synthesis recipes are still difficult to reproduce from one laboratory to the other under apparently the same conditions and that several adjustments are sometimes required.[19−21,25] A common reason for such lack of reproducibility can be sought in the different purities of the chemicals used in the synthesis, in the purification steps of the intermediate products in a multistep synthesis, or even in the apparatus used. The incomplete removal or the accidental introduction of unknown impurities can be responsible for the irreproducibility in the syntheses and is a factor that is often difficult to track down.

A possible source of impurity is represented by halide ions. They can be present in trace amounts in the surfactants used in the synthesis, in the solvents used to clean the products of a given synthesis, as residual species in NCs for which metal halides were used as precursors, and as species adsorbed on glassware or even on the magnetic stir bars, as a result of standard cleaning procedures. Halide ions interact strongly with

* Address correspondence to liberato.manna@iit.it.

Received for review October 22, 2012 and accepted November 24, 2012.

Published online November 26, 2012
10.1021/nn3048846

Scheme 1. Typical evolution of the CdSe/CdS multipod shape when large molar fractions of $CdCl_2$ are introduced in the synthesis of core−shell CdSe/CdS NCs, starting from $Cu_{2-x}Se$ as seeds. After the cation exchange reaction, during which the $Cu_{2-x}Se$ NCs are converted into CdSe NCs, octapods are first generated. Soon, however, in many of these octapods, the four pods with sharp tips start receding and eventually disappear. The other group of pods instead keeps growing, such that many NCs are reshaped into tetrapods.

cadmium chalcogenides. A few groups have reported on the role of halide ions on both growth and structural transformation of cadmium chalcogenide NCs.[26−30] Zou *et al.*, for example, observed shape and phase changes of CdS NCs by cationic surfactants in non-injection syntheses.[26] They proposed that the strong binding between Cd^{2+} and halide ions reduced the reactivity of the precursors and was responsible for the decrease in the number of nuclei formed in the nucleation stage, while maintaining at the same time a high concentration of precursors in the growth stage. These factors overall resulted in the increase of average size and in phase transformation of the CdS NCs. Lim *et al.* studied size and shape control of Cd chalcogenide NCs by chemical and photochemical etching methods in Cl^--containing solvents.[27,28] Cl^- ions, generated either by chemical activation of chloromethane with tributylphosphine or by photoinduced electron transfer from NCs to chloromethane molecules adsorbed on the NC surface, were the active species that induced anisotropic reshaping of the NCs. Saruyama *et al.* developed a method for drastic structural transformation of cadmium chalcogenide NCs through an Ostwald ripening process induced by Cl^- and by the surfactants.[29] The dissolution of Cd halides from the surface of the NCs generated reactive ligand-free sites on the surface of the NCs, which facilitated a ripening process.

One class of materials that can suffer the most from the presence of unknown impurities is that of anisotropic NCs, such as nanorods, nanowires, and branched NCs, whose synthesis often depends on a delicate balance of parameters. In previous works from us, we reported, for example, on the synthesis of octapod-shaped NCs.[31] These were prepared by injecting a solution of berzelianite $Cu_{2-x}Se$ NCs with tri-*n*-octylphosphine sulfide (TOPS) into a flask in which previously CdO had been mixed with tri-*n*-octylphosphine oxide (TOPO) and with phosphonic acids, namely, *n*-octadecylphosphonic acid (ODPA) and *n*-hexylphosphonic acid (HPA), and heated.[31] Upon injection, the $Cu_{2-x}Se$ NCs underwent exchange of Cu^+ ions with Cd^{2+} ions, and the resulting sphalerite CdSe NCs acted as seeds for the growth of CdSe/CdS octapods. The synthesis could also be carried out in two steps: first, CdSe NCs were prepared by cation exchange from $Cu_{2-x}Se$, then these were injected together with TOPS in the flask, as described above.[31] However, repeated tests in our laboratories, following both paths, have shown that the synthesis of octapods suffers from reproducibility issues, leading in many cases to the formation of CdS rods together with nanoparticles of a variety of other shapes.

In this work, we have studied the influence of chloride ions on the synthesis of branched CdSe/CdS core/shell NCs. When seeking a more robust approach to the synthesis of branched NCs with high yields, we found that, by deliberately adding chloride ions (Cl^-) in the reaction, *via* the introduction of the Cd precursor as a mixture of CdO and $CdCl_2$, the synthesis of octapods became fully reproducible. $CdCl_2$ was chosen as additive also because it is used extensively in the semiconductor industry as etchant and promoter of grain recrystallization and growth, as well as Cl doping agent, especially in CdTe-based solar cells, to improve cell performance.[32,33] In our experiments, octapods were obtained when working with molar fractions of $CdCl_2$ (over the total amount of Cd precursor added) around 0.06, which represents a fairly low amount of $CdCl_2$. Also, the octapod shape was stable during the synthesis course, even if this was run for 1 h. Furthermore, experimental conditions could be finely tuned such that the pod lengths in these octapods could be varied from 30 to about 50 nm, by using mixtures of alkylphosphonic acids of various chain lengths, in different molar ratios.

An additional finding of our experiments was that, for larger fractions of $CdCl_2$ added, octapods still formed at the early stages of the synthesis, but many of them tended to reshape into tetrapods over the reaction time (Scheme 1). In this case, we could isolate the intermediate products of the transformation: these were octapods with one group of four pods (departing at tetrahedral angles from each other and characterized by sharp tips) which were shorter than the other group of four pods. Eventually, the first group of pods disappeared, while the other group of pods kept growing. Such shape evolution might be due to an additional role of Cl-containing species in influencing the relative stabilities of various crystal facets of the CdS pods, perhaps by selective adhesion to certain sets of facets or yet by selective etching.

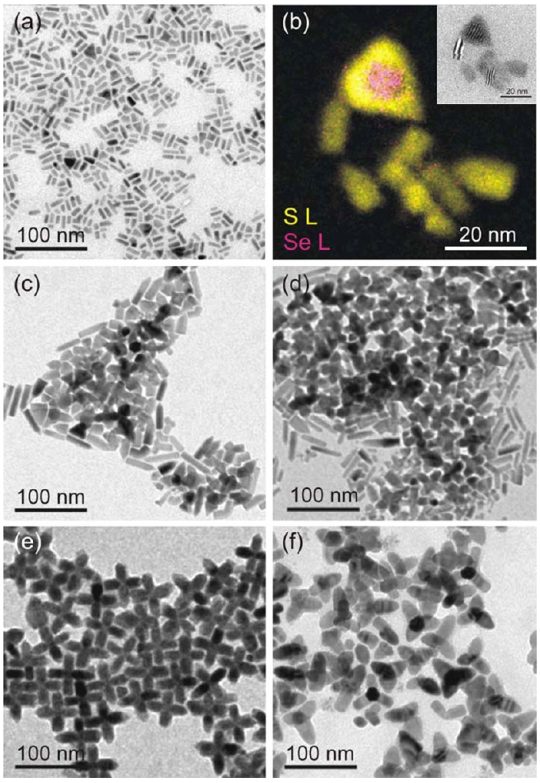

Figure 1. TEM images of NCs synthesized by using mixtures of CdO and $CdCl_2$ as Cd precursors, with f_{CdCl_2} equal to (a) 0.00, (c) 0.02, (d) 0.04, (e) 0.06, and (f) 0.32. (b) Combination of EFTEM elemental maps of S (yellow) and Se (magenta) of a group of NCs from the same sample as shown in (a). The inset in (b) is the corresponding zero-loss TEM image. In (e), the octapods appear often as "Greek crosses" because four pods, touching the support film, are overlapped in projection with the other four pods pointing upward.

RESULTS AND DISCUSSION

Results of Syntheses Carried out at Various Molar Fractions of $CdCl_2$. To survey the influence of $CdCl_2$ on the synthesis of NCs, different amounts of $CdCl_2$ and CdO were mixed in a flask containing TOPO, ODPA, and HPA. The one-step synthesis of octapods was performed, namely, $Cu_{2-x}Se$ seeds co-injected with TOPS in the flask underwent *in situ* cation exchange to CdSe. Then, on top of these NCs, CdS was grown. The total amount of Cd introduced was held fixed at 0.5 mmol, and all other reaction parameters were kept constant, too. For example, the overall molar ratio of phosphonic acids (HPA + ODPA) to Cd stayed fixed at 2.7:1. The results of the syntheses performed with molar fraction of $CdCl_2$ (f_{CdCl_2} = moles$_{CdCl_2}$/(moles$_{CdCl_2}$ + moles$_{CdO}$)) ranging from 0.00 to 0.32 are summarized in Figure 1. These are transmission electron microscopy (TEM) images of the NCs as synthesized, with no size-selective precipitation. All syntheses were run for 10 min.

When no $CdCl_2$ was added, the main product of the synthesis often consisted of nanorods, along with minor fractions of tetrahedral-shaped particles (Figure 1a). The nanorods were made only of CdS, while the tetrahedral particles were core/shell CdSe/CdS NCs, as assessed by both energy-filtered TEM (EFTEM) and energy-dispersive X-ray spectroscopy (EDS) elemental analysis (see Figures 1b and S1 of the Supporting Information). It is clear that the nanorods were formed by homogeneous nucleation in solution, while the core/shell structures were the result of heterogeneous nucleation of CdS on the starting seeds, after their conversion to CdSe. When working at low f_{CdCl_2} (0.02−0.04), the resulting products were mixtures of nanorods, tetrahedral particles, tripods, tetrapods (Figure 1c,d), along with a few octapods (especially in Figure 1d). When f_{CdCl_2} was increased to 0.06, the only products formed were octapods consisting of sphalerite CdSe and wurtzite CdS, as identified by powder X-ray diffraction (XRD) (Figure 1e; see also Figure S2 of Supporting Information). Fundamentally similar results were obtained in a two-step synthesis of octapods (Figure S3 of Supporting Information), consisting of first obtaining CdSe from $Cu_{2-x}Se$, cleaning the particles, and then injecting them in a second flask. At higher f_{CdCl_2} (for example, 0.32, Figure 1f), mainly tetrapods were found. Similar results were obtained when working at even higher f_{CdCl_2} (see Figure S4 of Supporting Information).

The results of these syntheses can be rationalized by considering that Cl species appear to reduce the availability of Cd in solution. This occurs most likely *via* formation of strong complexes with Cd and with the surfactants present. It is known that cadmium halides (CdX_2) react with phosphines (R_3P) and form complexes of the type $[CdX_2(R_3P)]_2$ and $[CdX_2(R_3P)_2]$,[34] and similar complexes are formed with phosphine oxides.[35] In principle, these complexes might be used as Cd precursors in the synthesis of colloidal NCs. Lazell *et al.* were able indeed to dissolve $CdCl_2$ in a mixture of TOP and TOPS, and the resulting solution was injected into TOPO to form CdS NCs.[36] CdO (a popular precursor species for cadmium chalcogenide NCs) instead does not dissolve in TOP or in TOPO and requires acids to be solubilized (which frees H_2O as a byproduct). Typical acids in this case are fatty acids and phosphonic acids. Cd phosphonates or carboxylates are then good Cd precursors as they can release cadmium in solution under suitable conditions. On the other hand, when Qu *et al.* tested $CdCl_2$ instead of CdO as precursor in the presence of fatty acids or phosphonic acids,[37] they could not synthesize CdSe NCs but did obtain only a few bulk crystals. They concluded that, under these conditions, cadmium formed complexes that were too strong, which reduced the rate of nucleation in solution considerably. Also, tests carried out in our lab demonstrated that, when $CdCl_2$ is dissolved in a mixture of an alkylphosphonic acid and TOPO, Cl species remain in the solution and are not eliminated as hydrochloric acid (HCl; see Figure S5 of Supporting Information). It is likely that complexes involving mainly phosphonates and chloride ions are formed in

this case. Elucidating the nature of the complexes formed in the presence of $CdCl_2$ and fatty acids or phosphonic acids, including the case discussed in the present work, will require extensive purification and characterization studies. This is additionally complicated by the fact that the actual species operative at the high temperatures of the synthesis might very well differ in structure from those that can be analyzed at room temperature, after cooling the reaction mixture.

In our syntheses, when no $CdCl_2$ is purposely introduced in the system, the energetic barrier for homogeneous nucleation is apparently low, so that, in addition to growth of CdS on top of the CdSe seeds, side nucleation of separate CdS NCs takes place (Figure 1a,b). The large number of CdS NCs formed quickly deprives the system of Cd species and only thin CdS shells can grow on top of the CdSe seeds. For syntheses carried out at higher f_{CdCl_2}, less CdS rods are nucleated in solution and the fraction of branched NCs, with long pods, increases (Figure 1c–f). Under the present reaction conditions, stable growth of octapods is possible for f_{CdCl_2} around 0.06 (Figure 1e). Then, for higher values of f_{CdCl_2}, the synthesis becomes unstable again: while branched NCs are still the major product formed, these are mainly tetrapods (Figure 1f).

Shape Evolution from Octapods to Tetrapods. To help rationalize the morphologies of Figure 1, especially those of Figure 1e,f, one must recall that such NCs were the products of syntheses that were run for 10 min. However, the particles might have undergone shape transformations during this time. It was interesting indeed to monitor the shape evolution for the two syntheses that yielded the most homogeneous samples in terms of shapes, that is, octapods, prepared at $f_{CdCl_2} = 0.06$ (Figure 1e) and tetrapods, prepared at $f_{CdCl_2} = 0.32$ (Figure 1f). For the two syntheses, aliquots were taken at different times from the injection and examined by TEM. The results are reported in Figure 2. In both cases, small octapods were formed within 30 s after seed injection. In the synthesis at $f_{CdCl_2} = 0.06$, the octapod shape persisted over the whole reaction course, with gradual increase in pod size (Figure 2, left panels). In this case, reaction conditions were such that all eight pods kept growing over time at the same rate, and therefore, the octapod shape remained stable over the time of the synthesis. Control experiments (see Figure S6 of Supporting Information) showed that the octapod shape persisted even in syntheses carried out for 1 h under these reaction conditions. On the other hand, in the synthesis performed at $f_{CdCl_2} = 0.32$, many of the initial octapods were reshaped into tetrapods and, over time, all NCs became fatter and developed bullet-shaped pods (Figure 2, right panels). Elemental mapping of the final NCs of this synthesis (see Figure S7 of Supporting Information) confirmed that the central region of these NCs was still CdSe.

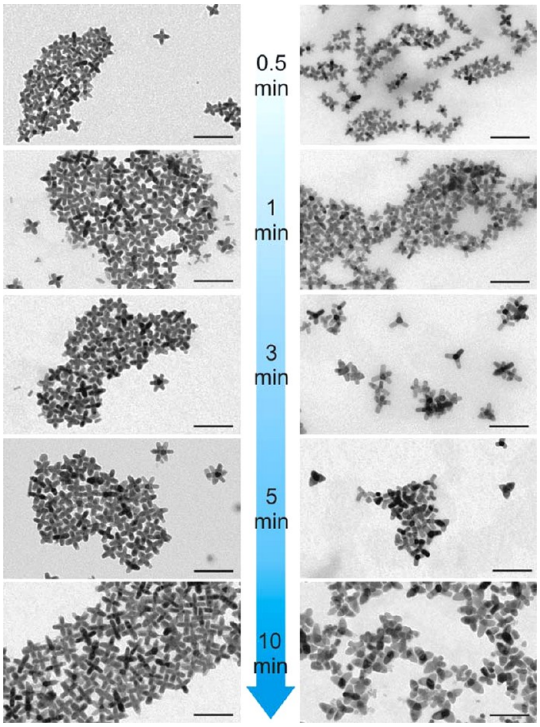

Figure 2. Sequences of TEM images (from top to bottom) of aliquots taken from syntheses run at $f_{CdCl_2} = 0.06$ (left panels) and $f_{CdCl_2} = 0.32$ (right panels). In the first case, the octapod shape was conserved throughout the synthesis course. In the second case, octapods evolved into tetrapods. Scale bars are 100 nm long.

A careful look at the aliquots of the synthesis with $f_{CdCl_2} = 0.32$, taken at 30 s and 1 min, explains how the shape transition occurred. Exemplary TEM images of individual NCs from these two samples are shown in Figure 3. In the aliquot at 30 s (Figure 3a, *i.e.*, top three rows), most particles were octapods with pod length more or less equal to each other. All pods were about 5 nm long on average. Already after 1 min, however, only four pods had grown considerably longer, those with relatively flat ends (to about 15–20 nm; see Figure 3b, *i.e.*, bottom three rows). The other four pods, characterized by sharp tips, had remained unchanged or had even receded in length. At this early stage, some particles had already become tetrapods, with little trace of the other four pods (see also Figure S8 of Supporting Information, which displays similar images for an aliquot taken at 5 min).

In this exemplary synthesis, octapods are formed at an early stage of the synthesis, but in many of these NCs, such shape evolved in the reaction environment. An explanation for this shape change might be sought if one considers that, in the octapods, one group of four CdS pods (evolving toward the [000–1] direction of wurtzite) has opposite polarity with respect to the other four pods (evolving in the [0001] direction of wurtzite), and therefore, the two groups of pods can undergo different shape evolution over time. This can be inferred especially by looking at the tip regions of

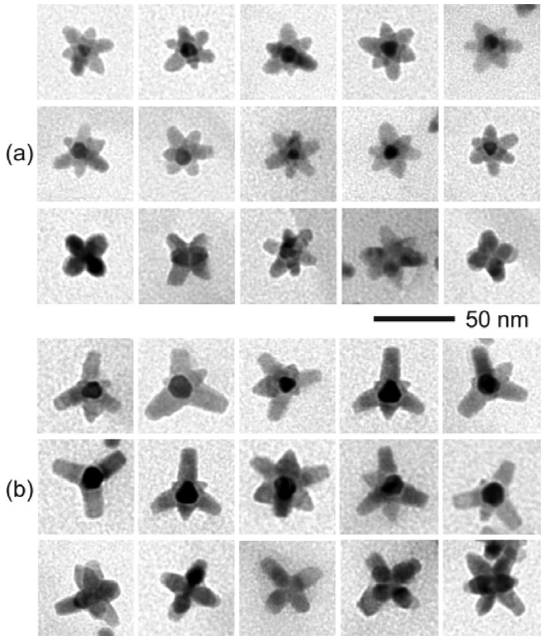

Figure 3. Aliquots of the synthesis run at f_{CdCl_2} = 0.32, taken at 30 s (a) and 1 min (b) after the injection. After 1 min, several "asymmetric" octapods were present. In these TEM images, most of the octapods are oriented such that two pods, one pointing upward and one pointing downward, are parallel to the electron beam: this orientation is possible for these particles due to the uneven length of opposite pods (*i.e.*, they lay on the support film with three of the longer pods touching it).

the various pods, in analogy to what was observed for simple rod-shaped wurtzite NCs, as discussed by us in previous works.[38,39] Indeed, the octapod can be thought as being composed of two interpenetrated tetrapods.[31,38,39] During reshaping, the pods with sharp tips (*i.e.*, the [000−1]-oriented ones)[31,38−40] stopped growing or they even receded, while the pods with initially flat ends kept growing. Most likely, the large concentration of Cl species present in this reaction influenced the growth rate and stability of the various facets, perhaps by selective adsorption to some facets or by preferential etching of some facets.[26−30] Then, for longer reaction time, further reshaping of the NCs took place, such that many of these tetrapods, as well as the surviving octapods, became fatter and developed bullet-shaped pods (see also Figures S7 and S8 of Supporting Information). It appears that, under these conditions, the presence of a high concentration of Cl species promoted also the lateral growth of the pods (hence their increase in diameter).

In order to check for the residual presence of chlorine species in the NC samples after they had been purified *via* several cleaning steps with toluene and methanol, we performed EDS analyses both by high-resolution scanning electron microscopy (HRSEM) and by TEM. These were run on NCs obtained at f_{CdCl_2} = 0.32, for the aliquot taken at 1 min after the injection (see above). Cl species were mainly detected on NCs, isolated or in groups (see Figure S9a,b of Supporting Information). X-ray photoelectron spectroscopy (XPS) analysis indicated that Cl is in the form of chlorides in the sample (see Figure S9c of Supporting Information). The Cl/Cd atomic ratios of quantitative analyses by EDS and XPS were below 5%. This appears to exclude the Cl signal as arising from free complexes. Whether Cl-containing species are actually bound to the surface of the NCs and in what form will require further experiments. If Cl species are indeed present on the surface of NCs, most likely, they are not there as individual Cl^- ions, but rather in conjunction with phosphonic acids: this can be inferred from TEM images of neighboring NCs, which suggest the presence of an organic passivating shell around each NC, as octapods are not touching each other (they would touch each other if Cl^- were the only ligands). These issues will need to be clarified with further investigations aiming at elucidating the exact nature of species bound to the surface of NCs. After that, one can envisage carrying out experimental and theoretical studies of selective adhesion of such species to the various facets of CdS.

Control Experiments. To support our hypothesis on the role of Cl ions on nucleation and growth, we carried out several control experiments. In one series of experiments, we wanted to test the effect of chlorine on the nucleation and growth of CdS NCs alone. In these experiments, run at various f_{CdCl_2}, no $Cu_{2-x}Se$ seeds were co-injected in the flask (see Figure S10 of Supporting Information). All conditions were the same as those for the samples of Figure 1. When going from no $CdCl_2$ added at all to increasing f_{CdCl_2}, the final product evolved from small monodisperse spheres of 6 nm in average diameter (no $CdCl_2$ added) to large bullets, 55 nm wide and 140 nm long (f_{CdCl_2} = 0.32). Most important, when f_{CdCl_2} increased from 0 to 0.32, the total number of NCs synthesized decreased from 1.02×10^{-5} to 3.95×10^{-9} M. Our interpretation of these data is that the larger f_{CdCl_2} was, the fewer nuclei were formed. Then, when few nuclei were formed, these then grew into big nanoparticles because they suffered less competition for the remaining Cd^{2+} species. The peculiar evolution in shape, from spheres to straight rods and finally to bullets, can be due again to a shape directing effect of the Cl^- ions, as in the case of the shape evolution from octapods to tetrapods discussed earlier. Similar effects were also observed in control experiments involving this time nucleation and growth of CdSe NCs (see Figure S11 of Supporting Information), although differences among the various conditions were less marked than for CdS. All of these control experiments confirm an enhancement of lateral growth when a relatively high concentration of Cl^- ions is present in the synthesis environment.

We also tested other reaction conditions, as an alternative to addition of $CdCl_2$, for promoting the

growth of octapods. These included working at higher ratio of alkylphosphonic acid to Cd, adding phosphonic acids with shorter alkyl chains, and also performing syntheses at lower or higher reaction temperatures (instead of 380 °C). Exemplary control experiments in which these parameters are varied are reported in the Supporting Information (see Figures S12–S14). Although in some cases we could identify alternative conditions for synthesizing octapods, even in the best cases (see, for example, Figure S13b), the obtained NCs were not of quality comparable to octapods that were prepared when simply dosing $CdCl_2$ and CdO as precursors (for example, they had irregularly shaped pods and often the samples contained additional byproducts).

Furthermore, other control experiments were run in which alternative chlorine precursors (HCl or NaCl) were introduced in the synthesis instead of $CdCl_2$. In these syntheses, mixtures of NCs with a wide variety of shapes were formed, including rods of various lengths and tetrapods (or multipods) with very long pods (see Figures S15 and S16 of Supporting Information). To summarize, $CdCl_2$ brings the most reliable results among several chlorine sources for the octapod synthesis, although reactions carried out using NaCl or HCl would require further experiments to disentangle the influence of acidity or of the counterion from that of the added halide ions.

Tuning the Length of the Pods. Overall, the reaction scheme identified in this work allowed us to find stable conditions for the growth of uniform octapod-shaped CdSe/CdS NCs, which appear to be critically dependent on the amount of $CdCl_2$ introduced. Once this issue was addressed, we could focus on other parameters that affect the overall morphology of the octapods. For example, we performed a series of syntheses in which we kept f_{CdCl_2} constant to an optimal value of 0.06 and also the ratio of total moles of phosphonic acids to moles of Cd (2.7:1). What we varied instead was the relative molar percentages of three different alkyl phosphonic acids as surfactants in addition to TOP and TOPO, namely, ODPA, HPA, and propyl phosphonic acid (PPA). Some results of the syntheses are summarized in Figure 4, along with TEM images of a few representative samples. A more complete set of data is reported in Figures S17 and S18 of the Supporting Information.

Remarkably, when using only one type of acid, results were never as good, in terms of sample uniformity, as when using mixtures of acids. Particularly, the phosphonic acids HPA and PPA, having short alkyl chains (C_3 and C_6, respectively), promoted the synthesis of octapods, while ODPA, with a C_{18} alkyl chain, yielded NCs with spheroidal shapes (Figure S17). Overall, by tuning the relative composition of the mixture of acids, we could tune the average length of the octapods from 30 to 50 nm. Further tuning might be possible by modifying other reaction conditions,[41−45]

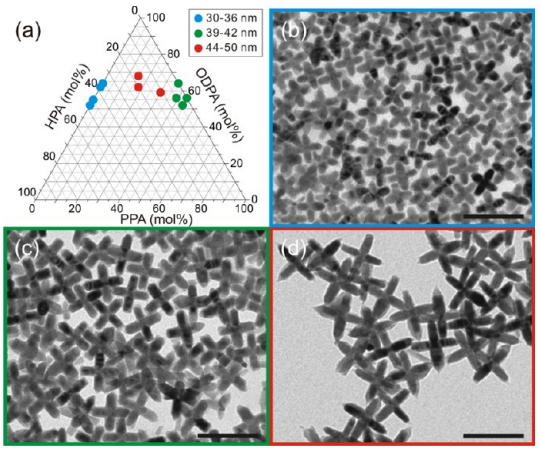

Figure 4. (a) Schematic diagram of the outcome of the experiments performed by varying the relative amounts of three different alkyl phosphonic acids (PPA, HPA, and ODPA), while keeping constant the ratio of total moles of phosphonic acids to moles of Cd (2.7:1) and also f_{CdCl_2} (0.06). In these experiments, we could fine-tune the pod lengths of the octapods. (b–d) Representative TEM images of octapods having pod lengths of (b) 33 nm, (c) 41 nm, and (d) 48 nm. Scale bars are 100 nm long in all panels. The color frames (blue, green, and red) of the panels are representative of each octapod group matched with colored dots in the diagram shown in (a). The ranges of average pod lengths are 30–36 nm (blue), 39–42 nm (green), and 44–50 nm (red). A more complete diagram with additional data points is reported in Figure S18 of Supporting Information.

for example, Cd/phosphonic acid ratio, growth temperature, amounts of seeds and precursors injected, and reaction time. All of these parameters can be easily tested in future works.

CONCLUSIONS

In conclusion, we have reported an approach to synthesize colloidal octapod-shaped CdSe/CdS NCs by carefully dosing the amount of $CdCl_2$ together with CdO as cadmium precursors, as well as fine-tuning of the pod length by varying the relative ratios of alkyl phosphonic acids. Moreover, in the presence of a relatively high amount of $CdCl_2$, we observed a shape evolution from octapods to tetrapods through asymmetric octapods. Such evolution might suggest a general scenario in the growth of branched NCs of II–VI semiconductors when looking, for example, in retrospect at various synthesis reports which were based on seeded growth approaches.[44−46] These started from cubic sphalerite seeds, on top of which pods of wurtzite phase were grown. In all of those syntheses, no formation of octapods was observed, but only tetrapods were reported. On the other hand, in our works on seeded-growth branched NCs, the use of relatively large seeds (10–15 nm in diameter) allowed the almost exclusive formation of octapods.[31,38] Is the initial size and shape of the seeds used by us (octahedra with all eight {111} facets well-developed) the only reason why we could access the octapod shape? On the basis of the present work, we can actually speculate that, in

some of the previously reported syntheses, octapods might have represented an early shape in the growth stage, whose evolution then to tetrapods might have occurred so early in the synthesis that the octapods' shape went actually undetected.

The availability of monodispersed octapods with tunable pod aspect ratio is indeed of major importance when their assemblies in tailored superstructures (1D, 2D, or 3D) are desired for specific applications.[47,48] Finally, asymmetric octapods, with four pods having dimensions and shapes much different from the other four pods, might uncover interesting opportunities for their shape-dependent optical and electronic properties and for their self-assembly behavior.

EXPERIMENTAL SECTION

Chemicals. Copper chloride (CuCl, 99.999%), tri-*n*-octylphosphine oxide (TOPO, 99%), tri-*n*-octylphosphine (TOP, 97%), and selenium (Se, 99.99%) were purchased from Strem Chemicals. Cadmium oxide (CdO, 99.99%), cadmium chloride ($CdCl_2$, 99.99%), sulfur (S, 99.98%), oleylamine (70%), 1-octadecene (90%), and (propyl)phosphonic acid (PPA, 95%) were purchased from Sigma-Aldrich. *n*-Octadecylphosphonic acid (ODPA) and *n*-hexylphosphonic acid (HPA) were purchased from Polycarbon Industries. Anhydrous methanol and toluene were purchased from Carlo Erba reagents. All chemicals were used as received.

Synthesis of $Cu_{2-x}Se$ NCs (Used as Seeds for Preparing Octapods). All procedures described here and in the next section were carried out using a standard Schlenk line. A copper precursor solution was prepared by adding 1 mmol of CuCl into a reaction flask containing 5 mL of oleylamine and 5 mL of octadecene. The mixture was heated under vacuum for 1 h at 80 °C and then heated to 300 °C under nitrogen flow. A selenium precursor solution was prepared by mixing 0.5 mmol of Se in 5 mL of oleylamine. The mixture was put under vacuum for 1 h at 130 °C, then it was heated to 230 °C under constant nitrogen flow, until Se was completely dissolved. At this point, it was cooled to 180 °C and then transferred into a glass syringe equipped with a stainless needle with a 12 gauge diameter in order to be injected quickly into the copper solution (kept at 300 °C). After injection, the reaction was kept at 300 °C for 15 min (counted from the moment of the injection). The flask was then cooled to room temperature. This synthesis yielded $Cu_{2-x}Se$ NCs with an average size of 15 nm. The NCs were then isolated and purified by repeated precipitation with methanol and redispersion in toluene. They were then dissolved in 3 mL of TOP. The NC concentrations of $Cu_{2-x}Se$ in TOP was determined to be around 3×10^{-6} M by inductively coupled plasma optical emission spectroscopy on digested solutions (with HCl/HNO_3 3:1 (v/v)).

Synthesis of CdSe/CdS Nanocrystals. The synthesis of octapods was modified with respect to those described in previous works by our group.[31,47] For the various syntheses reported here and in the Supporting Information, the various amounts of CdO, $CdCl_2$, and phosphonic acids are reported in Table S1 of the Supporting Information. Given amounts of CdO, $CdCl_2$, and phosphonic acids and 3 g of TOPO were loaded in a reaction flask and then heated to 120 °C under vacuum for 1 h. The mixture was heated to 380 °C under nitrogen flow, then 2.6 mL of TOP was injected, after which the temperature of the flask was allowed to recover to 380 °C. In the glovebox, 100 μL of a 3.0×10^{-6} M solution of $Cu_{2-x}Se$ NCs in TOP (corresponding, therefore, to 3.0×10^{-10} moles of NCs) was mixed with 0.5 g of TOPS (previously prepared by dissolving 96 mg of S in 1 mL of TOP). The resulting mixture was then injected rapidly into the reaction flask kept at 380 °C. After injection, the temperature of the flask was allowed to recover to 380 °C, and the reaction was run for 10 min (counted from the moment of the injection). We also carried out a two-step synthesis of octapods: the first step consisted of just transforming the $Cu_{2-x}Se$ seeds to CdSe NCs by exchanging Cu^+ ions with Cd^{2+} ions. In this case, the procedure was the same as that reported above for the synthesis of octapods, except that in this case the solution injected contained only $Cu_{2-x}Se$ seeds dissolved in TOP, with no TOPS. The overall reaction time after injection was 10 min, after which is was cooled to room temperature. The CdSe NCs were purified by repeated washings with toluene and methanol and redispersed in TOP. The second step was again the same as that reported above for the synthesis of octapods, except that in this case the solution injected contained, in addition to TOPS, 200 μL of a 1.1×10^{-6} M solution of CdSe NCs dissolved in TOP as obtained from the first step (instead of the $Cu_{2-x}Se$ seeds as in the one-step synthesis).

Characterization. Transmission electron microscopy (TEM) images were recorded by a JEOL JEM 1011 microscope operating at 100 kV. Energy-filtered TEM (EFTEM) elemental maps and scanning TEM high-angle annular dark-field (STEM-HAADF) images were recorded on a JEOL JEM 2200FS instrument operating at 200 kV, equipped with a CEOS image aberration corrector and an in-column energy filter (Ω filter). The EFTEM maps were acquired with the three-window method at the S L core-loss edge (165 eV onset energy, 20 eV slit width) and at the Se L edge (1436 eV onset energy, 100 eV slit width). EDS analyses from selected areas were acquired in STEM-HAADF mode using a Bruker Quantax 400 system with a 60 mm^2 silicon drift detector (SDD). High-resolution scanning electron microscopy (HRSEM) images were obtained by a JEOL JSM 7500FA microscope, equipped with an Oxford X-Max 80 system with a SDD for EDS analyses. Powder X-ray diffraction (XRD) measurements were performed with a Rigaku SmartLab X-ray diffractometer using Cu Kα source (50 kV, 150 mA), and X-ray photoelectron spectroscopy (XPS) measurements were carried out on a Kratos Axis Ultra DLD spectrometer using a monochromatic Al Kα source (15 kV, 20 mA).

Conflict of Interest: The authors declare no competing financial interest.

Acknowledgment. The authors acknowledge financial support through the FP7 ERC starting grant NANO-ARCH (Contract No. 240111).

Supporting Information Available: Details on reagents involved in the various syntheses of NCs. Additional details on structural and compositional characterization. Control experiments. Additional details on tuning the pod lengths. This material is available free of charge *via* the Internet at http://pubs.acs.org.

REFERENCES AND NOTES

1. Talapin, D. V.; Lee, J. S.; Kovalenko, M. V.; Shevchenko, E. V. Prospects of Colloidal Nanocrystals for Electronic and Optoelectronic Applications. *Chem. Rev.* **2010**, *110*, 389–458.
2. Kamat, P. V. Quantum Dot Solar Cells. Semiconductor Nanocrystals as Light Harvesters. *J. Phys. Chem. C* **2008**, *112*, 18737–18753.
3. Gill, R.; Zayats, M.; Willner, I. Semiconductor Quantum Dots for Bioanalysis. *Angew. Chem., Int. Ed.* **2008**, *47*, 7602–7625.
4. Smith, A. M.; Nie, S. M. Semiconductor Nanocrystals: Structure, Properties, and Band Gap Engineering. *Acc. Chem. Res.* **2010**, *43*, 190–200.
5. Nozik, A. J.; Beard, M. C.; Luther, J. M.; Law, M.; Ellingson, R. J.; Johnson, J. C. Semiconductor Quantum Dots and Quantum Dot Arrays and Applications of Multiple Exciton Generation to Third-Generation Photovoltaic Solar Cells. *Chem. Rev.* **2010**, *110*, 6873–6890.

6. Krahne, R.; Morello, G.; Figuerola, A.; George, C.; Deka, S.; Manna, L. Physical Properties of Elongated Inorganic Nanoparticles. *Phys. Rep.* **2011**, *501*, 75–221.
7. Konstantatos, G.; Sargent, E. H. Nanostructured Materials for Photon Detection. *Nat. Nanotechnol.* **2010**, *5*, 391–400.
8. Jun, Y. W.; Choi, J. S.; Cheon, J. Shape Control of Semiconductor and Metal Oxide Nanocrystals through Nonhydrolytic Colloidal Routes. *Angew. Chem., Int. Ed.* **2006**, *45*, 3414–3439.
9. Kumar, S.; Nann, T. Shape Control of II–VI Semiconductor Nanomateriats. *Small* **2006**, *2*, 316–329.
10. Park, J.; Joo, J.; Kwon, S. G.; Jang, Y.; Hyeon, T. Synthesis of Monodisperse Spherical Nanocrystals. *Angew. Chem., Int. Ed.* **2007**, *46*, 4630–4660.
11. Rao, C. N. R.; Vivekchand, S. R. C.; Biswas, K.; Govindaraj, A. Synthesis of Inorganic Nanomaterials. *Dalton Trans.* **2007**, 3728–3749.
12. Rogach, A. L.; Franzl, T.; Klar, T. A.; Feldmann, J.; Gaponik, N.; Lesnyak, V.; Shavel, A.; Eychmuller, A.; Rakovich, Y. P.; Donegan, J. F. Aqueous Synthesis of Thiol-Capped CdTe Nanocrystals: State-of-the-Art. *J. Phys. Chem. C* **2007**, *111*, 14628–14637.
13. Kwon, S. G.; Hyeon, T. Colloidal Chemical Synthesis and Formation Kinetics of Uniformly Sized Nanocrystals of Metals, Oxides, and Chalcogenides. *Acc. Chem. Res.* **2008**, *41*, 1696–1709.
14. Zhang, Q.; Liu, S. J.; Yu, S. H. Recent Advances in Oriented Attachment Growth and Synthesis of Functional Materials: Concept, Evidence, Mechanism, and Future. *J. Mater. Chem.* **2009**, *19*, 191–207.
15. Grzelczak, M.; Perez-Juste, J.; Mulvaney, P.; Liz-Marzan, L. M. Shape Control in Gold Nanoparticle Synthesis. *Chem. Soc. Rev.* **2008**, *37*, 1783–1791.
16. Lim, B.; Xia, Y. N. Metal Nanocrystals with Highly Branched Morphologies. *Angew. Chem., Int. Ed.* **2011**, *50*, 76–85.
17. Donega, C. D. Synthesis and Properties of Colloidal Heteronanocrystals. *Chem. Soc. Rev.* **2011**, *40*, 1512–1546.
18. Jiang, Z. J.; Kelley, D. F. Role of Magic-Sized Clusters in the Synthesis of CdSe Nanorods. *ACS Nano* **2010**, *4*, 1561–1572.
19. Wang, F. D.; Tang, R.; Buhro, W. E. The Trouble with TOPO; Identification of Adventitious Impurities Beneficial to the Growth of Cadmium Selenide Quantum Dots, Rods, and Wires. *Nano Lett.* **2008**, *8*, 3521–3524.
20. Wang, F.; Tang, R.; Kao, J. L. F.; Dingman, S. D.; Buhro, W. E. Spectroscopic Identification of Tri-*n*-octylphosphine Oxide (TOPO) Impurities and Elucidation of Their Roles in Cadmium Selenide Quantum-Wire Growth. *J. Am. Chem. Soc.* **2009**, *131*, 4983–4994.
21. Wolcott, A.; Fitzmorris, R. C.; Muzaffery, O.; Zhang, J. Z. CdSe Quantum Rod Formation Aided by *In Situ* TOPO Oxidation. *Chem. Mater.* **2010**, *22*, 2814–2821.
22. Peng, Z. A.; Peng, X. G. Nearly Monodisperse and Shape-Controlled CdSe Nanocrystals *via* Alternative Routes: Nucleation and Growth. *J. Am. Chem. Soc.* **2002**, *124*, 3343–3353.
23. Manna, L.; Scher, E. C.; Alivisatos, A. P. Synthesis of Soluble and Processable Rod-, Arrow-, Teardrop-, and Tetrapod-Shaped CdSe Nanocrystals. *J. Am. Chem. Soc.* **2000**, *122*, 12700–12706.
24. Manna, L.; Milliron, D. J.; Meisel, A.; Scher, E. C.; Alivisatos, A. P. Controlled Growth of Tetrapod-Branched Inorganic Nanocrystals. *Nat. Mater.* **2003**, *2*, 382–385.
25. Hughes, B. K.; Luther, J. M.; Beard, M. C. The Subtle Chemistry of Colloidal, Quantum-Confined Semiconductor Nanostructures. *ACS Nano* **2012**, *6*, 4573–4579.
26. Zou, Y.; Li, D. S.; Yang, D. R. Shape and Phase Control of CdS Nanocrystals Using Cationic Surfactant in Noninjection Synthesis. *Nanoscale Res. Lett.* **2011**, *6*, 374.
27. Lim, S. J.; Kim, W.; Jung, S.; Seo, J.; Shin, S. K. Anisotropic Etching of Semiconductor Nanocrystals. *Chem. Mater.* **2011**, *23*, 5029–5036.
28. Lim, S. J.; Kim, W.; Shin, S. K. Surface-Dependent, Ligand-Mediated Photochemical Etching of CdSe Nanoplatelets. *J. Am. Chem. Soc.* **2012**, *134*, 7576–7579.
29. Saruyama, M.; Kanehara, M.; Teranishi, T. Drastic Structural Transformation of Cadmium Chalcogenide Nanoparticles Using Chloride Ions and Surfactants. *J. Am. Chem. Soc.* **2010**, *132*, 3280–3282.
30. Guo'an, T.; Jianxin, Z.; Wanlin, G. Inorganic Salt-Induced Phase Control and Optical Characterization of Cadmium Sulfide Nanoparticles. *Nanotechnology* **2010**, *21*, 175601.
31. Deka, S.; Miszta, K.; Dorfs, D.; Genovese, A.; Bertoni, G.; Manna, L. Octapod-Shaped Colloidal Nanocrystals of Cadmium Chalcogenides *via* "One-Pot" Cation Exchange and Seeded Growth. *Nano Lett.* **2010**, *10*, 3770–3776.
32. Komin, V.; Tetali, B.; Viswanathan, V.; Yu, S.; Morel, D. L.; Ferekides, C. S. The Effect of the $CdCl_2$ Treatment on CdTe/CdS Thin Film Solar Cells Studied Using Deep Level Transient Spectroscopy. *Thin Solid Films* **2003**, *431–432*, 143–147.
33. Riech, I.; Pena, J. L.; Ares, O.; Rios-Flores, A.; Rejon-Moo, V.; Rodriguez-Fragoso, P.; Mendoza-Alvarez, J. G. Effect of Annealing Time of $CdCl_2$ Vapor Treatment on CdTe/CdS Interface Properties. *Semicond. Sci. Technol.* **2012**, *27*, 045015.
34. McAuliffe, C. A.; Levason, W. *Phosphine, Arsine, and Stibine Complexes of the Transition Elements*; Elsevier Scientific: Amsterdam, 1979.
35. Jorge, R. A.; Airoldi, C.; Changas, A. P. Thermochemistry of Dichlorobis(triphenylphosphine oxide)-Zinc(II), -Cadmium(II), and -Mercury(II). *J. Chem. Soc., Dalton Trans.* **1978**, 1102–1104.
36. Lazell, M.; O'Brien, P. Synthesis of CdS Nanocrystals Using Cadmium Dichloride and Trioctylphosphine Sulfide. *J. Mater. Chem.* **1999**, *9*, 1381–1382.
37. Qu, L. H.; Peng, Z. A.; Peng, X. G. Alternative Routes toward High Quality CdSe Nanocrystals. *Nano Lett.* **2001**, *1*, 333–337.
38. Brescia, R.; Miszta, K.; Dorfs, D.; Manna, L.; Bertoni, G. Birth and Growth of Octapod-Shaped Colloidal Nanocrystals Studied by Electron Tomography. *J. Phys. Chem. C* **2011**, *115*, 20128–20133.
39. Bertoni, G.; Grillo, V.; Brescia, R.; Ke, X.; Bals, S.; Catellani, A.; Li, H.; Manna, L. Direct Determination of Polarity, Faceting, and Core Location in Colloidal Core/Shell Wurtzite Semiconductor Nanocrystals. *ACS Nano* **2012**, *6*, 6453–6461.
40. Miszta, K.; Dorfs, D.; Genovese, A.; Kim, M. R.; Manna, L. Cation Exchange Reactions in Colloidal Branched Nanocrystals. *ACS Nano* **2011**, *5*, 7176–7183.
41. Gomes, R.; Hassinen, A.; Szczygiel, A.; Zhao, Q. A.; Vantomme, A.; Martins, J. C.; Hens, Z. Binding of Phosphonic Acids to CdSe Quantum Dots: A Solution NMR Study. *J. Phys. Chem. Lett.* **2011**, *2*, 145–152.
42. Wang, W.; Banerjee, S.; Jia, S. G.; Steigerwald, M. L.; Herman, I. P. Ligand Control of Growth, Morphology, and Capping Structure of Colloidal CdSe Nanorods. *Chem. Mater.* **2007**, *19*, 2573–2580.
43. Qu, L. H.; Yu, W. W.; Peng, X. P. *In Situ* Observation of the Nucleation and Growth of CdSe Nanocrystals. *Nano Lett.* **2004**, *4*, 465–469.
44. Huang, J.; Kovalenko, M. V.; Talapin, D. V. Alkyl Chains of Surface Ligands Affect Polytypism of CdSe Nanocrystals and Play an Important Role in the Synthesis of Anisotropic Nanoheterostructures. *J. Am. Chem. Soc.* **2010**, *132*, 15866–15868.
45. Talapin, D. V.; Nelson, J. H.; Shevchenko, E. V.; Aloni, S.; Sadtler, B.; Alivisatos, A. P. Seeded Growth of Highly Luminescent CdSe/CdS Nanoheterostructures with Rod and Tetrapod Morphologies. *Nano Lett.* **2007**, *7*, 2951–2959.
46. Fiore, A.; Mastria, R.; Lupo, M. G.; Lanzani, G.; Giannini, C.; Carlino, E.; Morello, G.; De Giorgi, M.; Li, Y.; Cingolani, R.; *et al.* Tetrapod-Shaped Colloidal Nanocrystals of II–VI Semiconductors Prepared by Seeded Growth. *J. Am. Chem. Soc.* **2009**, *131*, 2274–2282.
47. Miszta, K.; de Graaf, J.; Bertoni, G.; Dorfs, D.; Brescia, R.; Marras, S.; Ceseracciu, L.; Cingolani, R.; van Roij, R.; Dijkstra, M.; *et al.* Hierarchical Self-Assembly of Suspended

Branched Colloidal Nanocrystals into Superlattice Structures. *Nat. Mater.* **2011**, *10*, 872–876.
48. Qi, W.; de Graaf, J.; Qiao, F.; Marras, S.; Manna, L.; Dijkstra, M. Ordered Two-Dimensional Superstructures of Colloidal Octapod-Shaped Nanocrystals on Flat Substrates. *Nano Lett.* **2012**, *12*, 5299–5303.